Computer Assisted Mechanics and Engineering Sciences, **17**: 75–88, 2010.
Copyright © 2010 by Institute of Fundamental Technological Research, Polish Academy of Sciences

Transient heat conduction by different versions of the Method of Fundamental Solutions – a comparison study

Jan A. Kołodziej
Institute of Applied Mechanics, Poznan University of Technology
ul. Piotrowo 3, 60-965 Poznan, Poland
e-mail: jan.kolodziej@put.poznan.pl

Magdalena Mierzwiczak
Institute of Applied Mechanics, Poznan University of Technology
ul. Piotrowo 3, 60-965 Poznan, Poland
e-mail: magdalena.mierzwiczak@wp.pl

(Received in the final form September 14, 2010)

The computational accuracy of three versions of the method of fundamental solutions (MFS) is compared. The first version of MFS is based on the Laplace transformation of the governing differential equations and of the boundary conditions. The second version of MFS is based on the fundamental solution of the governing differential equation and discretization in time. The third method approximates the temperature time derivative by finite difference scheme. As the test problems the 2D boundary-initial-value problems (2D_BIVP) in square rectangular region Ω with known exact solutions are considered. Our numerical experiments show that all discussed methods achieve relatively accurate approximate solution but the third one offers less computational complexity and better efficiency.

Keywords: method of fundamental solutions, meshless method, transient heat conduction, initial-boundary volume problem, boundary collocation method

1. Introduction

The problem of transient conduction appears in diverse areas of science and technology and has been extensively treated in the literature. The time duration of the transient part can be important in the design of machine such as turbines. For the majority, the analytical solutions can not be found and the numerical solution is preferred. The domain type numerical methods such as finite difference and finite element methods are not necessarily the best approaches because their mesh character. Another alternative is application of boundary element method with dual reciprocity which converts domain integrals onto a series of boundary integral, see e.g. [1]. In this paper, a much simpler approach based on a method of fundamental solutions (MFS) is presented. The method discussed here gives the solution anywhere inside the region and on the boundary.

The method of fundamental solutions, as one version of the Trefftz method, has become increasingly popular over the last two decades. The majority of the applications of this method pertain to the elliptic problems [2]. However, in recent years some different versions of the MFS used for parabolic heat transfer problems have appeared [3–11]. In paper [3] two version of MFS for 2-D parabolic problem with zero initial conditions have been proposed: 1) method based on the Laplace transformation of the governing equation and the boundary condition, 2) method with time dependent fundamental solutions. For the inverse of Laplace transformation the method proposed in paper [12] has been used. The MFS based on the Laplace transformation for non-zero initial condition was proposed in paper [4]. The particular solution of non-homogeneous Helmholtz equation was

obtained by method suggested by Atkinson [13], while for inverse Laplace transformation Stehfest's algorithm [14] was used. In paper [5] for transient heat conduction with non-zero initial condition two versions of MFS have been proposed: 1) method based on Laplace transformation, 2) method in which finite difference scheme was used for time derivative. In both cases it leads to sequence of non-homogeneous Helmholtz equations. The particular solution of non-homogeneous Helmholtz equation was obtained by method proposed in paper [15]. In paper [6] the MFS based on the Laplace transformation for unsteady heat conduction equation with constant initial conditions have been discussed. For the inverse of Laplace transformation the method proposed in paper [12] has been used. Papers [7] and [9] discussed the MFS with time dependent fundamental solution for the non-zero initial conditions. In paper [10] this version of MFS was applied for diffusion equation with heat sources. In all the papers discussed so far a 2-D initial value problem was considered, with the exception of paper [8] in which 3-D diffusion equation was considered. In paper [8] the authors used a version based on finite difference scheme for time derivative, transforming the original parabolic equation into a sequence of non-homogeneous modified Helmholtz equations.

As even this short review shows, three different versions of the MFS applied to transient heat conduction problem are now available. The first one is a version of MFS based on the Laplace transformation of the governing differential equations and of the boundary conditions. The second version of MFS is based on the fundamental solution of the governing differential equation and discretization in time. The third method approximates the temperature time derivative by finite difference scheme. Some comparison of second and third version of MFS is given in paper [11] but this author for comparison purpose uses only one exact solutions with three different combinations of boundary conditions.

The purpose of the present paper is to investigate computational accuracy of these three different versions of the MFS in application for transient heat conduction. Four examples for 2-D boundary-initial-value problem with exact solution are presented to demonstrate the efficacy of the proposed different versions of method. In a sense this paper is a continuation of paper [3] in which two versions of MFS have been compared with FEM for 2-D heat conduction problem. Main result of that paper concludes that at the same number of degrees of freedom the MFS is more accurate than FEM.

2. Problem statement

A two-dimensional homogeneous, isotropic region Ω with boundary $\partial\Omega$ is considered. The governing equation for unsteady Fourier heat conduction in square region without the internal heat sources (our boundary-initial-value problem) is following

$$\frac{\partial \breve{T}}{\partial t}(x,y,t) = \alpha \nabla^2 \breve{T}(x,y,t) \quad \text{in} \quad \Omega = [0,1]\times[0,1], \tag{1}$$

$$\breve{T}(x,y,0) = g(x,y) \quad \text{in} \quad \Omega, \tag{2}$$

$$\breve{a}\cdot \breve{T}\left(x_B,y_B,t\right) + \breve{b}\cdot \frac{\partial \breve{T}\left(x_B,y_B,t\right)}{\partial n} = \breve{c} \quad \text{on} \quad \partial\Omega, \tag{3}$$

where α is the thermal diffusivity of the region (constant), $g(x,y)$ is the specified initial temperature distribution, x_B, y_B are coordinates of boundary points, n is outward normal to the boundary, $\breve{a}$, $\breve{b}$, $\breve{c}$ define the boundary conditions.

We introduce the nondimensional variables: $T = \frac{\breve{T}}{T_r}$, $X = \frac{x}{l}$, $Y = \frac{y}{l}$, $F = \frac{\alpha t}{l^2}$, $G = \frac{g}{T_r}$, $a = \breve{a}$, $b = \frac{\breve{b}}{l}$, $c = \frac{c}{T_r}$. Then the governing equation and boundary and initial conditions (1–3) can be written in nondimensional form (see Fig. 1)

$$\frac{\partial T}{\partial F}(X,Y,F) = \nabla^2 T(X,Y,F) \quad \text{in} \quad \Omega = [0,1]\times[0,1], \tag{4}$$

$$T(X,Y,0) = G(X,Y) \quad \text{in} \quad \Omega, \tag{5}$$

$$a \cdot T\left(X_B, Y_B, F\right) + b \cdot \frac{\partial T\left(X_B, Y_B, F\right)}{\partial n} = c \quad \text{on} \quad \partial\Omega, \tag{6}$$

where $T(X, Y, F)$ is dimensionless temperature, $\nabla^2(\ldots) = \partial^2(\ldots)/\partial X^2 + \partial^2(\ldots)/\partial Y^2$ is the Laplace operator, F is Fourier number, $G(X, Y)$ is the specified dimensionless initial temperature distribution, X_B, Y_B are coordinates of boundary points, n – outward normal to the boundary, a, b, c define the boundary conditions.

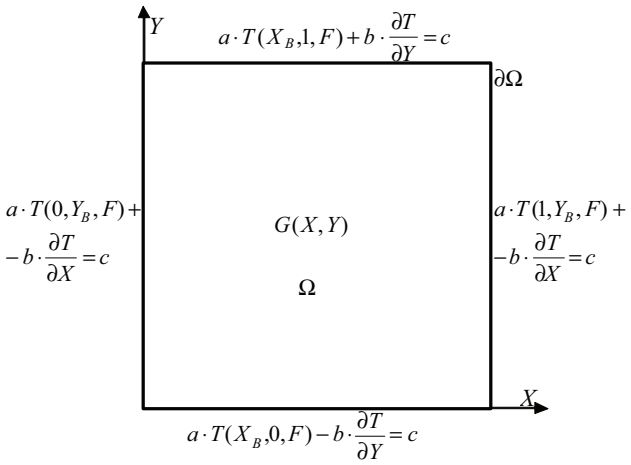

Fig. 1. Square region with dimensionless initial and boundary conditions

Three different methods of fundamental solutions can be used for solving the initial-boundary volume problem formulated by Eq. (4), the initial condition (5) and the boundary condition (6).

3. Numerical analysis

3.1. MFS with the Laplace transformation (MFS_L)

The first version of MFS is based on the Laplace transformation of the governing differential equations and of the boundary conditions [3–6].

Using the Laplace transformation the initial-boundary value problem has been transformed to inhomogeneous Helmholtz boundary value problem in the Laplace transfer domain (the s-domain)

$$\nabla^2 \bar{T}(X, Y, s) - s\bar{T}(X, Y, s) = -G(X, Y) \quad \text{in} \quad \Omega, \tag{7}$$

where $\bar{T}(X, Y, s)$ is the Laplace transform of $T(X, Y, F)$ with respect to Fourier number

$$\bar{T}(X, Y, s) = \int_0^\infty e^{-sF} T(X, Y, F)\, dF. \tag{8}$$

The Laplace transform of the boundary condition in Eq. (3) has the form

$$a \cdot \bar{T}\left(X_B, Y_B, s\right) + b \cdot \frac{\partial T\left(X_B, Y_B, s\right)}{\partial n} = c. \tag{9}$$

In accordance with the MFS, the general approximate solution of Eq. (7) is a sum $\bar{T} = \bar{T}^{(h)} + \bar{T}^{(p)}$ of homogeneous solution $\bar{T}^{(h)}$

$$\nabla^2 \bar{T}^{(h)}(X, Y, s) - s\bar{T}^{(h)}(X, Y, s) = 0, \tag{10}$$

and particular solution $\bar{T}^{(p)}$ of inhomogeneous equation

$$\nabla^2 \bar{T}^{(p)}(X,Y,s) - s\bar{T}^{(p)}(X,Y,s) = -G(X,Y). \tag{11}$$

The radial basis functions (RBF) and polynomials are used in order to obtain a particular solution of Eq. (11). The unknown coefficients are determined from the interpolation of the right hand side

$$-G(X,Y) = \sum_{j=1}^{M} a_j \varphi\left(r_j\right) + \sum_{k=1}^{L} b_k p_k(X,Y), \tag{12}$$

where $r_j = \sqrt{(X-X_j)^2 + (Y-Y_j)^2}$, $\varphi\left(r_j\right) = r_j^2 \ln\left(r_j\right)$ is one of the radial basis functions known as thin plate spline, (X_j, Y_j), $j = 1, \ldots, M$ are coordinates of equidistant interpolation points which are located inside the region Ω, $p_k(X,Y)$ are polynomials given in Table 1, M is number of interpolation points and $L = 6$ is a number of polynomials.

Table 1. Polynomial functions with their particular solutions

k	$p_k(X,Y)$	$q_k(X,Y)$
1	1	$-1/s$
2	X	$-X/s$
3	Y	$-Y/s$
4	XY	$-XY/s$
5	X^2	$-X^2/s - 2/s^2$
6	Y^2	$-Y^2/s - 2/s^2$

After determination of the coefficients a_j and b_k particular solution of Eq. (7) has form

$$T^{(p)}(X,Y) = \sum_{j=1}^{M} a_j \psi\left(r_j\right) + \sum_{k=1}^{L} b_k q_k(X,Y), \tag{13}$$

where functions $\psi\left(r_j\right)$ and $q_k(X,Y)$ are solutions of equations

$$\nabla^2 \psi\left(r_j\right) - s\psi\left(r_j\right) = \varphi\left(r_j\right), \qquad j = 1, \ldots, M, \tag{14}$$

$$\nabla^2 q_k(X,Y) - s q_k(X,Y) = p_k(X,Y), \qquad k = 1, \ldots, L. \tag{15}$$

Functions q_k are given in Table 1, whereas function $\psi\left(r_j\right)$ takes form

$$\psi\left(r_j\right) = \begin{cases} -\frac{4}{s^2}\left(K_0\left(\sqrt{s}r_j\right) + \ln\left(r_j\right) + 1\right) - \frac{r_j^2 \ln(r_j)}{s} & \text{for } r_j > 0, \\ \frac{4}{s^2}\left(\gamma + \ln\left(\frac{\sqrt{s}}{2}\right) - 1\right) & \text{for } r_j = 0, \end{cases} \tag{16}$$

where $\gamma \approx 0,57722$ is Euler's constant. The approximate homogeneous solution of Eq. (10) is a superposition of the modified Bessel function of the second kind and zero order with unknown coefficients W_j

$$\bar{T}(X,Y,s) = \sum_{j=1}^{NS} W_j K_0\left(\sqrt{s}\sqrt{(X-X_j)^2 + (Y-Y_j)^2}\right), \tag{17}$$

where (X_j, Y_j), $j = 1, \ldots, NS$ are coordinates of source points which are located outside the region Ω at a distance S from the boundary, NS is number of source points. In the MFS approach the unknown coefficients W_j are designated from the collocation boundary condition (9) for each value

of s [16]. The known values of the coefficients allow to find the transformed field of temperature, which may later be inverted to the nondimensional time domain

$$\bar{T}(X,Y) = \sum_{j=1}^{NS} W_j K_0 \left[\sqrt{s}\sqrt{(X-X_j)^2+(Y-Y_j)^2}\right] + \sum_{j=1}^{M} a_j \psi\left(r_j\right) + \sum_{k=1}^{L} b_k q_k(X,Y). \tag{18}$$

Once obtained, the transformed solution in defined N field points with the desired solution must be inverted back to time domain.

The proper solution in the considered domain is assumed as a function of Fourier number [17]

$$T(F) = A + BF + \sum_{j=1}^{NS} C_j \exp\left(-D_j F\right). \tag{19}$$

These unknown coefficients A, B, C_j, D_j are evaluated by taking the Laplace transform of Eq. (19) and by comparing this equation and the general approximate solution for parameter s

$$s\bar{T}(s) = A + \frac{B}{s} + \sum_{j=1}^{NS} \frac{C_j}{1+\frac{D_j}{s}}. \tag{20}$$

This procedure is applied for each N domain point in order to recover the solution at different values of time. The known values of coefficients A, B, C_j, D_j for each point allow finding the value of temperature at different time step using Eq. (19).

3.2. MFS with collocation space and time (MFS_C)

The second version of MFS is based on the fundamental solution of the governing differential equation (4) [3, 7, 8, 10]. The approximate solution Eq. (4) is expressed as linear superposition of these fundamental solutions and has the form

$$T(X,Y,F) = \sum_{j=1}^{NS}\sum_{l=0}^{Nt-1} T_j\left(l\Delta F\right) \frac{\exp\left(-\frac{(X-X_j)^2+(Y-Y_j)^2}{4(F-l\Delta F)}\right)}{4\pi\left(F-l\Delta F\right)}, \tag{21}$$

where (X_j, Y_j) are coordinates of outside source points which are located outside the region Ω at a distance S from the boundary, ΔF is inclement of Fourier number, $F = Nt\Delta F$ is Fourier's number and $T_j(l\Delta F)$ is a value of temperature in previous time step. Equation (21) satisfies governing equation (4) exactly for all (X, Y, F).

It can be shown that an initial temperature distribution is equivalent to an infinite number of infinitesimal internal heat sources, which release momentary blasts of heat at time $F = 0$ only, and in amounts sufficient to raise their temperatures to the specified initial conditions. By following the same reasoning for the MFS, the solution is the sum of contributions from M known internal sources and from NS unknown external sources

$$\begin{aligned} T(X,Y,F) = &\sum_{k=1}^{M} G\left(X_k,Y_k\right)\left[\frac{\exp\left(-\frac{(X-X_k)^2+(Y-Y_k)^2}{4F}\right)}{4\pi F}\right]\Delta A_k \\ &+ \sum_{j=1}^{NS}\sum_{l=0}^{Nt-1} T_j(l\Delta F)\left[\frac{\exp\left(-\frac{(X-X_j)^2+(Y-Y_j)^2}{4(F-l\Delta F)}\right)}{4\pi(F-l\Delta F)}\right], \end{aligned} \tag{22}$$

where ΔA_k is the region into domain with centered heat inside source point (X_k, Y_k), $k = 1/\ldots, M$, $F = Nt\Delta F$, NS is the number of heat sources outside the boundary and M is the number of heat sources inside the region representing the initial temperature distribution. The unknowns $T_j(l\Delta F)$ are determined from collocation of boundary conditions (5) at each time step.

3.3. MFS with finite difference method (MFS_F)

Now there are many variants of finite difference methods for parabolic equation (4). In the third method we choose the θ-method. Let $\tau > 0$ be nondimensional time increment (step), and we define the mesh for time as $F_n = n\tau$, $n \geq 0$. For $F_n \leq F \leq F_{n+1}$, approximations for temperature $T(X, Y, F)$, Laplacian of temperature, and time derivatives of temperature are assumed in the form

$$T(X,Y,F) \cong \theta T\left(X,Y,F_{n+1}\right) + (1-\theta)T\left(X,Y,F_n\right), \tag{23}$$

$$\nabla^2 T(X,Y,F) \cong \theta \nabla^2 T\left(X,Y,F_{n+1}\right) + (1-\theta)\nabla^2 T\left(X,Y,F_n\right), \tag{24}$$

$$\frac{\partial T(X,Y,F)}{\partial F} \cong \frac{T\left(X,Y,F_{n+1}\right) - T\left(X,Y,F_n\right)}{\tau}. \tag{25}$$

where $0 \leq \theta \leq 1$. Using (24, 25) in (4) we have

$$\theta \nabla^2 T\left(X,Y,F_{n+1}\right) + (1-\theta)\nabla^2 T\left(X,Y,F_n\right) = \frac{T\left(X,Y,F_{n+1}\right) - T\left(X,Y,F_n\right)}{\tau}. \tag{26}$$

Introducing notation to $T\left(X,Y,F_n\right) = w_n(X,Y)$ and after algebraic manipulations, we have

$$\nabla^2 w_{n+1} - \frac{1}{\theta\tau} w_{n+1} = -\frac{1}{\theta\tau} w_n - \frac{1-\theta}{\theta}\nabla^2 w_n. \tag{27}$$

For $\theta = 1$ we get the backward difference scheme (MFS_F_B) [5, 9]

$$\nabla^2 w_{n+1} - \frac{1}{\tau} w_{n+1} = -\frac{1}{\tau} w_n, \tag{28}$$

and for $\theta = 0.5$ we get the Crank-Nicolson scheme (MFS_F_CN)

$$\nabla^2 w_{n+1} - \frac{2}{\tau} w_{n+1} = -\frac{2}{\tau} w_n - \nabla^2 w_n. \tag{29}$$

Now, one can notice that Eq. (27) is a sequence of inhomogeneous modified Helmholtz equations

$$\nabla^2 w_{n+1} - \lambda^2 w_{n+1} = f_n(X,Y), \tag{30}$$

where $\lambda^2 = 1/(\theta\tau)$, and at each time step F_{n+1} function $f_n(X,Y) = f\left(w_n, \nabla^2 w_n\right)$ is known from previous time step. For the first time step, we have $w_0(X,Y) = G(X,Y)$ from the initial condition. The solution of Eq. (26) $w_{n+1} = w_{n+1}^{(h)} + w_{n+1}^{(p)}$ is sum of the homogeneous solution $w_{n+1}^{(h)}$

$$\nabla^2 w_{n+1}^{(h)} - \lambda^2 w_{n+1}^{(h)} = 0, \tag{31}$$

and the particular solution $w_{n+1}^{(p)}$

$$\nabla^2 w_{n+1}^{(p)} - \lambda^2 w_{n+1}^{(p)} = f_n(X,Y). \tag{32}$$

The solution of the homogeneous equations (31) is a linear combination of fundamental solutions of the homogeneous modified Helmholtz equation with the coefficients determined from the collocation of boundary conditions at each time step

$$w_{n+1}^{(h)}(X,Y) = \sum_{j=1}^{NS} W_j K_0\left[\lambda\sqrt{(X-X_j)^2 + (Y-Y_j)^2}\right] = \sum_{j=1}^{NS} W_j K_0\left[\lambda r_j\right], \tag{33}$$

where (X_j, Y_j) are coordinates of source points which are located outside the region Ω.

For the solution of the inhomogeneous equations (32) the right hand side function $f_n(X,Y)$ must be interpolated by RBF and polynomials with unknown coefficients.

$$f_n(X,Y) = \sum_{j=1}^{M} a_j \varphi\left(r_j\right) + \sum_{k=1}^{L} b_k p_k(X,Y). \tag{34}$$

After determination of the coefficients a_j and b_k (see part MFS_L), the particular solution of Eq. (26) has a form of a linear combination of particular solution for RBF and polynomials

$$w_{n+1}^{(p)}(X,Y) = \sum_{j=1}^{M} a_j \psi(r_j) + \sum_{k=1}^{L} b_k q_k(X,Y). \tag{35}$$

At each time step the field of temperature is calculated by formula

$$T(X,Y,F) = \sum_{j=1}^{NS} W_j^F K_0\left[\lambda r_j\right] + \sum_{j=1}^{M} a_j^F \psi(r_j) + \sum_{k=1}^{L} b_k^F q_k(X,Y). \tag{36}$$

4. Numerical results for some examples of 2D_BIVP

In this section four examples of 2D_BIVP are numerically analyzed by three different versions of the MFS. In order to validate the discussed numerical methods, the four 2D examples chosen from literature with known exact solutions, are carried out. With the available values of the exact solution and the approximate solution from the numerical experiment for some control points ($NN = 400$) in the domain, the maximal relative error and the root mean squared relative error can be evaluated by

$$\delta_{MAX} = \frac{\max\limits_{1\le i\le NN}\left\{\left|T_{i,\,\text{ana.}} - T_{i,\,\text{num.}}\right|\right\}}{\max\limits_{1\le i\le NN}\left\{\left|T_{i,\,\text{ana.}}\right|\right\}} 100\%, \tag{37}$$

$$\delta_{RMSE} = \frac{\sqrt{\sum\limits_{i=1,\ldots,NN}\left(T_{i,\,\text{ana.}} - T_{i,\,\text{num.}}\right)^2}}{\sqrt{\sum\limits_{i=1,\ldots,NN} T_{i,\,\text{ana.}}^2}} 100\%. \tag{38}$$

In all the cases the considered domain is unit square $\Omega = [0,1] \times [0,1]$ and boundary and initial

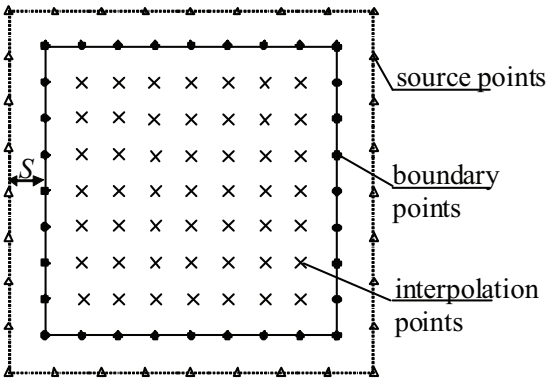

Fig. 2. Boundary (•), source (△), and interpolation (×) points

conditions are derived from the exact solution

$$\frac{\partial T}{\partial F}(X,Y,F) = \nabla^2 T(X,Y,F), \qquad 0 < X < 1, \qquad 0 < Y < 1.$$

On each unit segment of boundary ten equidistant collocation points are chosen and additional one point in each corner. The number of source points equals number of collocation points and they are placed on some contour geometrically similar to the contour of the boundary $\partial\Omega$. The distance between the contour of the boundary and the contour of sources equals 0.1. The distribution of collocation points ($NC = 44$), source points ($NS = 44$) and interpolation points ($M = 100$) in each of the versions of the boundary collocation were the same. These distributions are shown in Fig. 2.

4.1. First example of 2D_BIVP [8]

The analytical solution has form

$$T(X,Y,F) = \left(\cos\left(\frac{\pi X}{2}\right) + \cos\left(\frac{\pi Y}{2}\right) + \sin\left(\frac{\pi X}{2}\right) + \sin\left(\frac{\pi Y}{2}\right)\right) \exp\left(-\frac{\pi}{4}F\right).$$

The initial and boundary conditions are calculated from the analytical solution. The results ob-

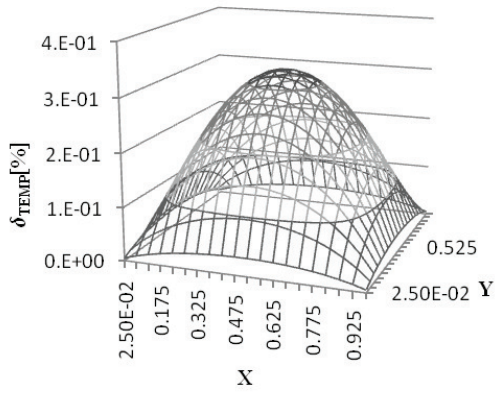

Fig. 3. Error of temperature field for the first example for MFS_F_B

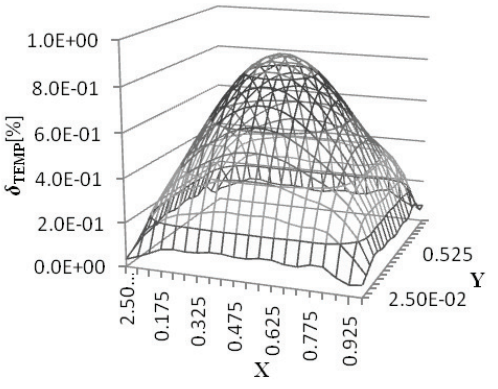

Fig. 4. Error of temperature field for the first example for MFS_C

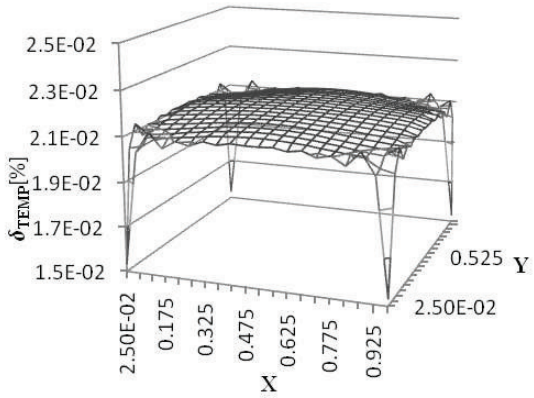

Fig. 5. Error of temperature field for the first example for MFS_L

tained for the first test example for $F = 0.3$ by means of three different versions of the MFS method, namely MFS_F_B, MFS_C and MFS_L, are presented in the form of the error of identification of the temperature field in Figs. 3 to 5, respectively. For the third version of MFS based on the backward difference scheme (MFS_F_B) the test of the influence the value of distance the source contour from the boundary contour S was carried out. As shown in Fig. 6 accuracy of the results does not depend significantly on the value of the parameter S.

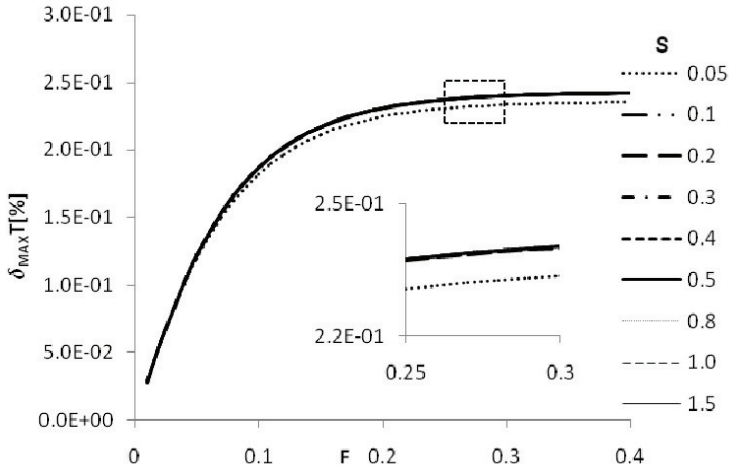

Fig. 6. The maximal error of temperature for MFS_C for the first test example and for different value of S

4.2. Second example [3]

The initial and boundary conditions:

$$T(X,Y,0) = 0, \qquad \frac{\partial T}{\partial X}(0,Y,F) = 0, \qquad T(1,Y,F) = -1,$$
$$\frac{\partial T}{\partial Y}(X,0,F) = 0, \qquad T(X,1,F) = -1.$$

The exact solution of this problem has the form

$$T(X,Y,F) = -1 + \frac{16}{\pi^2}\sum_{m=1}^{\infty}\sum_{n=1}^{\infty}\frac{(-1)^{m+n+2}\cos\left((2m-1)\pi\frac{X}{2}\right)\cos\left((2n-1)\pi\frac{Y}{2}\right)}{(2m-1)(2n-1)} \times \exp\left(-\left((2m-1)^2+(2n-1)^2\right)\pi^2\frac{F}{4}\right).$$

4.3. Third example with exact solution [7]

The initial and boundary conditions:

$$T(X,Y,0) = (1-X)(1-Y), \qquad T(0,Y,F) = 0, \qquad T(X,0,F) = 0,$$
$$T(X,1,F) = X, \qquad T(1,Y,F) = Y.$$

The exact solution can be obtained by separation of variables

$$T(X,Y,F) = XY + \sum_{i=1}^{\infty}\sum_{j=1}^{\infty} C_{ij}\sin(i\pi X)\sin(j\pi Y)\exp\left(-\pi^2\left(i^2+j^2\right)F\right),$$

where $C_{ij} = \frac{4}{ij\pi^2}\left(1-(-1)^{i+j}\right)$.

4.4. The last numerical example [18]

The initial conditions:

$$T(X,Y,0) = \cos\frac{\pi}{2}(X+Y) + \sin(X-Y).$$

The analytical solution:

$$T(X,Y,F) = \exp\left(-F\frac{\pi^2}{2}\right)\cos\frac{\pi}{2}(X+Y) + \exp\left(-2\pi^2 F\right)\sin(X-Y).$$

In Tables 2 to 5 the comparison of the values of the maximal relative error and the average

Table 2. Values of the maximal and the root mean squared relative error of temperature for the first example

F	MFS_L		MFS_C		MFS_F_B	
	δ_{MAX} [%]	δ_{RMSE} [%]	δ_{MAX} [%]	δ_{RMSE} [%]	δ_{MAX} [%]	δ_{RMSE} [%]
0.01	4.35E−02	4.34E−02	9.84E+01	7.27E+01	2.91E−02	2.28E−02
0.03	2.37E−02	2.35E−02	8.52E+01	4.91E+01	8.23E−02	5.76E−02
0.05	6.77E−03	6.53E−03	6.20E+01	3.39E+01	1.25E−01	8.29E−02
0.10	2.34E−02	2.39E−02	2.49E+01	1.34E+01	1.92E−01	1.20E−01
0.15	3.83E−02	3.90E−02	9.84E+00	5.29E+00	2.23E−01	1.37E−01
0.20	4.04E−02	4.13E−02	3.86E+00	2.07E+00	2.37E−01	1.45E−01
0.25	3.23E−02	3.34E−02	1.52E+00	8.32E−01	2.43E−01	1.49E−01
0.30	1.63E−02	1.77E−02	6.48E−01	3.94E−01	2.46E−01	1.51E−01
0.40	2.89E−02	2.70E−02	4.30E−01	3.08E−01	2.48E−01	1.52E−01
CPU time [s]	30.94		36.25		44.91	

Table 3. Values of the maximal and the root mean squared relative error of temperature for the second example

F	MFS_L		MFS_C		MFS_F_B	
	δ_{MAX} [%]	δ_{RMSE} [%]	δ_{MAX} [%]	δ_{RMSE} [%]	δ_{MAX} [%]	δ_{RMSE} [%]
0.01	2.88E+01	3.52E+01	3.65E+00	3.35E+00	1.72E+01	1.59E+01
0.03	6.58E+00	6.48E+00	6.96E+00	4.60E+00	6.79E+00	5.68E+00
0.05	1.02E+01	8.50E+00	8.01E+00	5.26E+00	4.25E+00	3.47E+00
0.1	1.03E+01	8.54E+00	9.56E+00	7.28E+00	2.03E+00	1.59E+00
0.15	5.94E+00	4.63E+00	1.80E+01	1.06E+01	1.19E+00	9.68E−01
0.20	2.12E+00	1.42E+00	2.71E+01	1.38E+01	1.18E+00	8.53E−01
0.25	2.11E+00	1.37E+00	3.42E+01	1.63E+01	1.48E+00	8.19E−01
0.30	3.89E+00	2.49E+00	3.92E+01	1.80E+01	1.51E+00	7.67E−01
0.40	5.05E+00	3.09E+00	4.49E+01	1.98E+01	1.30E+00	6.22E−01
CPU time [s]	128.78		134.79		142.08	

Table 4. Values of the maximal and the root mean squared relative error of temperature for the third example

F	MFS_L		MFS_C		MFS_F_B	
	δ_{MAX} [%]	δ_{RMSE} [%]	δ_{MAX} [%]	δ_{RMSE} [%]	δ_{MAX} [%]	δ_{RMSE} [%]
0.01	2.16E+01	2.99E+01	4.75E+01	6.57E+01	1.57E+01	1.58E+01
0.03	5.66E+00	5.88E+00	2.60E+01	3.69E+01	5.50E+00	7.13E+00
0.05	8.58E+00	1.20E+01	1.62E+01	2.26E+01	3.23E+00	4.33E+00
0.10	6.80E+00	9.58E+00	5.45E+00	7.51E+00	6.88E−01	9.14E−01
0.15	2.94E+00	4.11E+00	1.88E+00	2.65E+00	1.14E−01	1.52E−01
0.20	2.20E−01	2.59E−01	6.97E−01	1.16E+00	1.72E−02	2.28E−02
0.25	1.79E+00	2.50E+00	5.46E−01	8.46E−01	2.46E−03	3.26E−03
0.30	2.80E+00	3.92E+00	5.48E−01	7.87E−01	3.42E−04	4.53E−04
0.40	3.18E+00	4.45E+00	5.07E−01	7.33E−01	6.34E−06	8.41E−06
CPU time [s]	124.53		131.59		137.53	

Table 5. Values of the maximal and the root mean squared relative error of temperature for the fourth example

F	MFS_L		MFS_C		MFS_F_B	
	δ_{MAX} [%]	δ_{RMSE} [%]	δ_{MAX} [%]	δ_{RMSE} [%]	δ_{MAX} [%]	δ_{RMSE} [%]
0.01	1.59E+01	2.09E+01	5.88E+01	5.90E+01	8.42E−01	8.92E−01
0.03	4.83E+00	6.19E+00	2.75E+01	2.65E+01	1.86E+00	1.86E+00
0.05	4.87E+00	6.54E+00	1.25E+01	1.17E+01	2.19E+00	2.13E+00
0.10	1.86E+01	2.36E+01	2.42E+00	1.94E+00	1.70E+00	1.56E+00
0.15	1.85E+01	2.26E+01	1.61E+00	1.24E+00	9.52E−01	8.56E−01
0.20	9.84E+00	1.13E+01	1.33E+00	1.13E+00	5.00E−01	4.58E−01
0.25	4.93E+00	5.43E+00	1.14E+00	1.06E+00	2.99E−01	2.82E−01
0.30	1.86E+01	2.40E+01	9.82E−01	1.01E+00	2.38E−01	2.22E−01
0.40	4.96E+01	6.09E+01	1.10E+00	9.42E−01	2.21E−01	2.01E−01
CPU time [s]	31.51		35.79		44.28	

global relative error in calculation of field temperature for the three versions of MFS tested are presented. The calculations were carried out for time step equal 0.01. The analysis of the numerical results allows to state that for the majority of the test examples the MFS with approximation time derivative of temperature by backward difference scheme is the most exact. However, it should be noted that while for the first tested example (Table 2) the most exact is the version with the Laplace transformation, for the last case (Table 5) this method is divergent. As far as the collocation of space and time is concerned it can be concluded based on the results from Tables 2, 4 and 5 that it takes approximately about ten time steps for the method to become stable and guarantee correct results.

Table 6. Values of the root mean squared relative error of temperature for the first example

F	$\theta = 0.5$	$\theta = 0.6$	$\theta = 0.7$	$\theta = 0.8$	$\theta = 0.9$
0.01	1.05E+00	8.21E−01	6.08E−01	4.05E−01	2.10E−01
0.03	6.92E−01	5.60E−01	4.31E−01	3.04E−01	1.80E−01
0.05	4.87E−01	4.06E−01	3.25E−01	2.44E−01	1.63E−01
0.10	2.05E−01	1.91E−01	1.76E−01	1.59E−01	1.40E−01
0.15	8.68E−02	9.96E−02	1.11E−01	1.21E−01	1.30E−01
0.20	3.75E−02	6.05E−02	8.29E−02	1.05E−01	1.25E−01
0.30	8.36E−03	3.68E−02	6.53E−02	9.39E−02	1.22E−01
0.40	3.67E−03	3.24E−02	6.20E−02	9.18E−02	1.22E−01
CPU time [s]	44.83	44.89	44.79	44.82	44.86

5. Testing θ-method

It is necessary to evaluate the influence of value parameter θ used in the third version of MFS on the accuracy of the results. For testing θ-method the parameter θ is chosen from interval $0.5 \leq \theta \leq 1$. The results for the two first examples in the form of the root mean squared relative error of identification field of temperature for each time step for different value parameter θ are shown in Table 6 and 7. The results show that the accuracy of numerical solutions is dependent on the value θ.

Table 7. Values of the root mean squared relative error of temperature for the second example

F	$\theta = 0.5$	$\theta = 0.6$	$\theta = 0.7$	$\theta = 0.8$	$\theta = 0.9$
0.01	3.44E+01	2.96E+01	2.54E+01	2.18E+01	1.86E+01
0.03	7.01E+00	6.29E+00	5.98E+00	5.80E+00	5.70E+00
0.05	3.65E+00	3.47E+00	3.39E+00	3.36E+00	3.39E+00
0.1	1.52E+00	1.49E+00	1.47E+00	1.48E+00	1.52E+00
0.15	1.04E+00	1.02E+00	9.95E−01	9.77E−01	9.67E−01
0.2	8.24E−01	8.31E−01	8.37E−01	8.42E−01	8.47E−01
0.3	5.52E−01	5.92E−01	6.34E−01	6.78E−01	7.22E−01
0.4	3.76E−01	4.19E−01	4.67E−01	5.18E−01	5.70E−01
CPU time [s]	139.67	139.87	141.33	139.76	139.76

The smallest value of the root mean squared relative error for approximation temperature field in first time step has been obtained for $\theta = 1$, that is for the backward difference scheme (MFS_F_B).

With the increasing number of time steps the best results have been obtained for the smaller values of parameter θ. After the 20-th time step the most accurate is the Crank-Nicolson scheme (MFS_F_CN), where $\theta = 0.5$.

6. Conclusions

The paper presents three different versions of the MFS for solving transient heat conduction problem in 2-D unit domain. The first version is MFS with the Laplace transformation, the second is MFS with collocation of space and time and the last version uses the backward difference scheme. For all these methods the temperatures can be computed in a whole domain.

From presented results the following conclusion can be drawn:

- three different versions of the MFS for solving transient heat conduction problem in 2-D unit square domain were presented,
- for all these methods the temperatures can be computed in a whole domain,
- the numerical results show that all versions give acceptable results with respect to the root mean squared relative error,
- the worst method with respect to maximal relative error calculated at initial time is the second method, namely the method with time dependent fundamental solutions,
- the results demonstrate that MFS with backward difference scheme is the simplest and the best method for calculation of the field temperature.

Acknowledgments

First author made this work in frame of a Grant 3143/T02/2007 from the Polish Ministry of Higher Education.

The authors would like to thank the reviewers for their constructive comments on the first version of this article.

References

[1] R. Białecki, P. Jurgaś, G. Kuhn. Dual reciprocity BEM without matrix inversion for transient heat conduction. *Engineering Analysis with Boundary Elements*, **26**: 227–236, 2002.

[2] G. Fairweather, A. Karageorghis. The method of fundamental solutions for elliptic boundary value problems. *Advances in Computational Mathematics*, **9**: 69–95, 1998.

[3] J.A. Kołodziej, J. Stefaniak, M. Kleiber. Transient heat conduction by boundary collocation methods and FEM – a comparison study. In: W. Hackbusch, ed., *Numerical Techniques for Boundary Element Methods: Proceedings of the Seventh GAMM-Seminar*, Kiel, January 25–27, 1991. Published in: *Notes on Numerical Fluid Mechanics*, **33**, pp.104–115, 1992.

[4] C.S. Chen, M.A. Golberg, Y.C. Hon. The method of fundamental solutions and quasi-Monte-Carlo method for diffusion equations. *International Journal for Numerical Methods in Engineering*, **43**: 1421–1435, 1998.

[5] M.A. Golberg, C.S. Chen, A.S. Muleshkov. The method of fundamental solutions for time-dependent problems, In: C.S. Chen C.A. Brebia, D.W. Pepper, eds., *Boundary Element Technology XIII*, pp. 377–386, WIT Press, Southampton, 1999.

[6] E. Mahajerin, G. Burgess. A Laplace transform-based fundamental collocation method for two-dimensional transient heat flow. *Applied Thermal Engineering*, **23**: 101–111, 2003.

[7] G. Burgess, E. Mahajerin. Transient heat flow analysis using the fundamental collocation method. *Applied Thermal Engineering*, **23**: 893–904, 2003.

[8] D.L. Young, C.C. Tsai, K. Murugesan, C.M. Fan, C.W. Chen. Time-dependent fundamental solution for homogeneous diffusion problems. *Engineering Analysis with Boundary Elements*, **28**: 1463–1473, 2004.

[9] M.S. Ingber, C.S. Chen, J.A. Tanski. A mesh free approaches using radial basis functions and parallel domain decomposition for solving three-dimensional diffusion equations. *International Journal for Numerical Methods in Engineering*, **60**: 2183–2201, 2004.

[10] C.F. Dong. An extended method of time-dependent fundamental solutions for inhomogeneous heat conduction. *Engineering Analysis with Boundary Elements*, **33**: 717–725, 2009.

[11] S. Chantasiriwan. Methods of fundamental solutions for time-dependent heat conduction problems. *International Journal for Numerical Methods in Engineering*, **66**: 147–165, 2006.

[12] R.A. Schapery. Approximation methods of transform inversion for viscoelastic stress analysis. *Proceedings of the Fourth US National Congress on Applied Mechanics*, **2**: 1075–1085, 1962.
[13] K.E. Atkinson. The numerical evaluation of particular solution for Poisson's equation. *IMA J. Numer. Anal.*, **5**: 319–338, 1985.
[14] H. Stehfest. Algorithm 368: Numerical Inversion of the Laplace Transformation. *Communications of the ACM*, **13**: 47–49, 1970.
[15] M.A. Golberg, C.S. Chen, Y.F. Rashed. The annihilator method for computing particular solutions to partial differential eqautions. *Engineering Analysis with Boundary Elements*, **23**: 267–274, 1999.
[16] J.A. Kołodziej, A.P. Zieliński. *Boundary Collocation Techniques and their Application in Engineering.* WIT Press, Southampton 2009.
[17] B. Davies, B. Martin. Numerical inversion of Laplace Transform: a Survey and Comparison of Methods. *Journal of Computational Physics*, **33**: 1–32, 1979.
[18] J. Kouatchou. Comparison of time and spatial collocation methods for the heat equation. *Journal of Computational and Applied Mathematics*, **150**: 129–141, 2003.